Studies of parametrically excited non-linear MDOF systems at parametric resonances

T J Kniffka[1], B R Mace[2], H Ecker[1] and R Halkyard[2]

[1] Institute of Mechanics and Mechatronics, TU Wien, Getreidemarkt 9, 1060 Vienna, AT
[2] Department of Mechanical Engineering, University of Auckland, 20 Symonds Street, Auckland, NZ

E-mail: till.kniffka@tuwien.ac.at

Abstract. An increasing number of MEMS devices use parametric excitation (PE) to outperform conventional designs. These systems are operated at parametric resonance. Different to standard cases of resonance, at parametric resonances the vibration's amplitudes increase faster and within a smaller interval. The amplification is much larger and only limited by non-linearities. So far the focus has mostly been on one degree of freedom (1DOF) systems. This is partly caused by a lack of methods to investigate and design multi degree of freedom (MDOF) systems time-efficiently. Restricting the systems to 1DOF ignores the opportunity to make use of PE effects only available in MDOF systems: parametric combination resonances and parametric anti-resonances, where an enhanced damping behaviour can be observed. The paper demonstrates how to approximate non-linear MDOF PE systems with 1DOF models. This leads to a generalised, dimensionless model applicable to many systems. Approaches are presented for investigating such a reduced non-linear 1DOF PE model analytically and semi-analytically at parametric resonances using averaging methods. For a 2DOF system the results are validated numerically by continuation methods and time simulations. Limits of both the analytical and the semi-analytical approaches are discussed.

1. Introduction

In contrast to external excitation, such as force excitation or base excitation for example, parametric excitation (PE) means that parameters of the system vary over time. If this variation is time-periodical and its angular frequency Ω_{PE} is

$$\Omega_{\mathrm{PR},i,n} = \frac{2\omega_i}{n}, \quad \forall\, n \in \mathbb{N} \tag{1}$$

the rest position's steady state is destabilised. This effect is called parametric resonance (PR). Here ω_i is a natural angular frequency of the system. Considering multi degree of freedom (MDOF) systems also parametric combination resonances (PCRs) exist for PE frequencies of

$$\Omega_{\mathrm{PCR},ij,n} = \frac{\omega_i + \omega_j}{n}, \quad \forall\, n \in \mathbb{N}, \tag{2}$$

where ω_i and ω_j both are natural angular frequencies of the system. In addition, for MDOF systems it is possible not only to destabilise the rest position but also to enhance the energy

dissipation and therefore bring the system to rest faster from a perturbed state at certain PE frequencies

$$\Omega_{\mathrm{PAR},ij,n} = \frac{|\omega_i - \omega_j|}{n}, \quad \forall\, n \in \mathbb{N}. \tag{3}$$

This effect was first discovered by Tondl [1] and is called parametric anti-resonance (PAR). The phenomenon is caused by periodically shifting energy between the modes i and j. Thus the higher modal damping of the higher mode is exploited more effectively [2].

Compared to conventional resonance cases the instability intervals at PRs and PCRs are much more narrow. The change from the unstable rest position to a stable bifurcated limit cycle is instant in the frequency domain. The amplitudes of these limit cycles are only limited by non-linearities. The vibrations' amplitudes increase exponentially over time instead of linearly over time as for conventional resonance cases. For many applications PE holds possibilities to outperform conventional systems (see [3, 4, 5] for exaple). However, such systems are complicated to investigate analytically: the governing equations do not only have time varying terms, but also have to contain terms non-linearly depending on state variables. Without them amplitudes would increase indefinitely at PRs. Yet, analytical investigations are essential to understand the effects of the system parameters. Numerical investigations only yield specific results for the corresponding system which do not lead to a general understanding of the behaviour at PR. Hence, so far most applications are limited to 1DOF which leaves advantageous effects of PCRs and PARs unexploited.

In section 2 first a MDOF non-linear PE system is modelled in section 2.1 and then reduced to a 1DOF model in section 2.2. Its governing equations' solutions are approximated analytically and semi-analytically in section 2.3. These results are validated with results by numerical continuation in section 3.2. Section 4 summarises the findings and points out the practical value.

The parameter values (see table A1) of the system presented clearly refer to a micro system. In fact, the research leading to the results expounded here was motivated by microelectromechanical systems (MEMSs) for energy harvesting, weighing micro masses and filtering electric signals [3, 6, 7, 8]. Yet, this work targets non-linear MDOF PE systems in general and is not limited to certain applications. To the contrary, the results help to understand and to design any system which is operated at PR.

2. Investigating MDOF non-linear PE systems analytically

In this section a MDOF system is investigated analytically and semi-analytically at PR by first approximating it by a 1DOF model and then estimating the model's behaviour at PR using an averaging method.

2.1. Modelling MDOF non-linear PE systems

Multiple rigid bodies having masses m_i are coupled to each other via springs with non-linear stiffness parameters $k_{ij}(x_{ij})$ and viscoelastic dampers with damping constants c_{ij} (see figure 1). The system undergoes PE by the time-periodic stiffness constants $k_i(x_i, t)$.

The stiffness parameters are

$$k_{ij}(x_i, x_j) = k_{ij,\mathrm{lin}} + k_{ij,\mathrm{nlin}}(x_i - x_j)^2, \tag{4a}$$

$$k_i(x_i, t) = k_{\mathrm{PE},i}(x_i)(1 + \cos(\Omega_{\mathrm{PE}} t)), \tag{4b}$$

$$k_{\mathrm{PE},i}(x_i) = k_{\mathrm{PE},i,\mathrm{lin}} + k_{\mathrm{PE},i,\mathrm{nlin}} x_i^2. \tag{4c}$$

Hence the equations of motion become

$$\mathbf{M}\ddot{\mathbf{x}} + \mathbf{C}\dot{\mathbf{x}} + \mathbf{K}(\mathbf{x})\mathbf{x} + \mathbf{K}_{\mathrm{PE}}(\mathbf{x}) \cos(\Omega_{\mathrm{PE}} t)\mathbf{x} = \mathbf{0}, \tag{5}$$

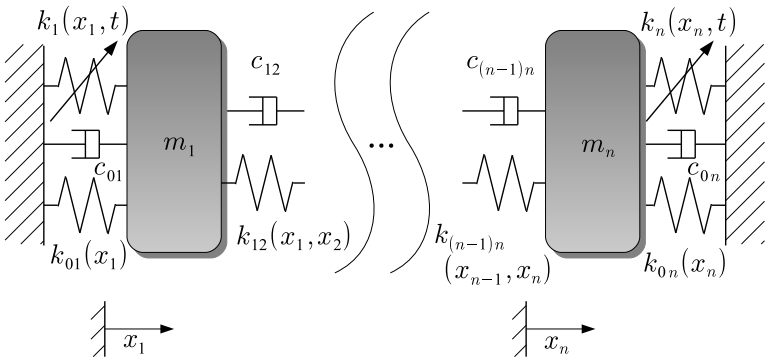

Figure 1. MDOF lumped mass model. The system is parametrically excited by springs with time-periodic stiffness constants $k_i(x_i,t)$.

where the abbreviation $\dot{(\,)} = \frac{\mathrm{d}}{\mathrm{d}t}$ denotes a time derivative. The mass matrix $\mathbf{M}$ and the PE matrix $\mathbf{K}_{\mathrm{PE}}(\mathbf{x})$ are diagonal. The stiffness matrix $\mathbf{K}(\mathbf{x})$ and the damping matrix $\mathbf{C}$ are fully occupied. Assuming the system to be proportionally damped, the damping matrix $\mathbf{C} = \alpha\mathbf{M} + \beta\mathbf{K}_{\mathrm{lin}}$ is a superposition of the mass matrix $\mathbf{M}$ and the linear part $\mathbf{K}_{\mathrm{lin}}$ of the stiffness matrix $\mathbf{K}(\mathbf{x})$.

Having defined $k_i(x_i,t)$ as stated in equation 4b makes the stiffness matrix $\mathbf{K}(\mathbf{x})$ depend on the PE stiffness constants $k_{\mathrm{PE},i,\mathrm{lin}}$ and $k_{\mathrm{PE},i,\mathrm{nlin}}$. This means the values of the linear PE stiffness constants $k_{\mathrm{PE},i,\mathrm{lin}}$ influence the system's natural frequencies. In contrast, the values of the linear PE stiffness constants $k_{\mathrm{PE},i,\mathrm{nlin}}$ influence the system's qualitative behaviour at PRs (as shown in section 2.4). This most general approach is chosen to govern a larger number of PE systems. However, for many systems the PE can be modelled using $k_i(x_i,t) = k_{\mathrm{PE},i}(x_i)\cos(\Omega_{\mathrm{PE}}t)$. Hence the system's natural frequencies and the system's qualitative behaviour at PRs become independent of the intensity of the PE.

2.2. Quasi-modal reduction

Setting $\mathbf{K}_{\mathrm{PE}} = \mathbf{0}$ in equation 5 describes the autonomous behaviour of the system. Solving the eigenvalue problem for such modified equation 5 the system's natural undamped angular frequencies ω_i and the corresponding modes $\boldsymbol{\varphi}_i$ are calculated. These modes can be normalised such that

$$\boldsymbol{\varphi}_i^{\mathrm{T}}\mathbf{M}\boldsymbol{\varphi}_i = 1 \tag{6}$$

and combined in the modal matrix $\boldsymbol{\phi} = [\boldsymbol{\varphi}_1\ \boldsymbol{\varphi}_2\ \ldots\ \boldsymbol{\varphi}_n]$.

Thus the displacement vector $\mathbf{x}$ can be transformed into the *quasi-modal* displacements $\mathbf{z}$ by $\mathbf{x} = x^*\boldsymbol{\phi}\mathbf{z}$. Here, x^* is a scaling parameter which is employed for having dimensionless quasi-modal displacements $\mathbf{z}$ as well as to provide a sufficient scaling for evaluating the differential equations numerically. The expression quasi-modal is used because $\mathbf{z}$ are the modal displacements for an autonomous set of differential equations. For a linear, time-invariant system these modal displacements are the amplitudes of the natural modes and the natural frequencies ω_i are the undamped vibration frequencies of the natural modes. In addition, for such a linear, time-invariant system the differential equations are decoupled.

For $\mathbf{K}_{\mathrm{PE}} \neq \mathbf{0}$ equation 5 cannot be decoupled. Yet, for a PE system the quasi-modal displacements z_i describe the vibration at PR regarding each mode. For simplification a normalisation is introduced regarding the eigentime $\tau = \Omega_{\mathrm{PE}}t$ and the dimensionless PE frequency $\Omega = \frac{\Omega_{\mathrm{PE}}}{\Omega^*}$ where Ω^* is some reference frequency. Applying the above transformation leads to

$$\mathbf{z}'' + \mathbf{Z}\mathbf{z}' + \boldsymbol{\Lambda}\mathbf{z} + \boldsymbol{\Lambda}_{\mathrm{nlin}}(\mathbf{z})\mathbf{z} + \mathbf{E}(\mathbf{z})\cos(\tau)\mathbf{z} = \mathbf{0}. \tag{7}$$

Here $\mathbf{\Lambda}$ is the normalised modal matrix with the elements $\frac{\omega_i^2}{\Omega^2}$ along its diagonal. The normalised modal damping matrix $\mathbf{Z}$ also is of diagonal shape and contains the elements $2\zeta_i\frac{\omega_i}{\Omega}$. Due to the assumption of proportional damping the modal damping can be calculated by

$$\zeta_i = \frac{\alpha}{2\omega_i} + \frac{\beta\omega_i}{2}. \tag{8}$$

Both matrices $\mathbf{\Lambda}_{\mathrm{nlin}}(\mathbf{z})$ and $\mathbf{E}(\mathbf{z})$ are fully occupied and their elements are quadratic and bilinear functions of $\mathbf{z}$.

As stated above the quasi-modal transformation means that each equation of the matrix equation 7 describes the vibration of one mode. At PR mainly the mode i is excited which corresponds to the PR frequency $\Omega_{\mathrm{PR},n} = \frac{2\omega_i}{n}$. Likewise, for PCRs with the centre frequency $\Omega_{\mathrm{PCR},n} = \frac{\omega_i+\omega_j}{n}$ both modes i and j are excited (see [9, 10] for example). With this knowledge, equation 7 can be approximated for PRs. The predominantly excited mode i has an amplitude much larger than all other modes which allows the quadratic and bilinear terms in $\mathbf{\Lambda}_{\mathrm{nlin}}(\mathbf{z})$ and $\mathbf{E}(\mathbf{z})$ to be set to zero except for terms containing z_i^2. This reduces the multi-dimensional problem of equation 7 to a scalar one, i.e.

$$z_i'' + 2\zeta_i\frac{\omega_i}{\Omega}z_i' + \left(\frac{\omega_i^2}{\Omega^2} + \frac{\epsilon_{i,\mathrm{lin}}}{\Omega^2}\cos(\tau)\right)z_i + \left(\frac{\kappa_i^2}{\Omega^2} + \frac{\epsilon_{i,\mathrm{nlin}}}{\Omega^2}\cos(\tau)\right)z_i^3 = 0, \tag{9}$$

where the linear and non-linear PE parameters $\epsilon_{i,\mathrm{lin/nlin}}$ determine the PE amplitude and the non-linearity parameter κ_i^2 condenses normalised non-linear stiffness parameters. However, such an approximation is only valid at the corresponding PR. The n-DOF system is approximated by n 1DOF systems—one for each mode. The n bodies of the MDOF system undergo vibrations which can be estimated by

$$x_k = \sum_{l=1}^{n}\varphi_{lk}z_l \approx \varphi_{ik}z_i \tag{10}$$

for the kth body. Here i indicates the quasi-mode $\boldsymbol{\varphi}_i$ and φ_{ik} is its kth element.

2.3. Averaging the non-linear 1DOF model's equation of motion

Employing the Krylov-Bogolyubov method (see [11] for example) equation 9 can be averaged over one period $\frac{2\pi}{\eta}$ of $z_i(\tau)$. Here the frequency ratio is $\eta = \frac{\omega_i}{\Omega_0}$ and Ω_0 is the centre frequency of the PR. For each mode's first PR ($n = 1 \Rightarrow \max(\Omega_{\mathrm{PR},n})$) this frequency ratio takes the value $\eta = \frac{1}{2}$. The deviation of the normalised PE angular frequency from Ω_0 is assumed to be very small, i.e.

$$\Omega = \Omega_0 + \Delta\Omega + \mathcal{O}(\Delta\Omega^2),\ \mathcal{O}(\Delta\Omega^2) \ll \Delta\Omega. \tag{11}$$

Introducing the amplitude r_i and the phase shift ψ_i for the quasi-modal displacement z_i equation 9 can be averaged for $\eta = \frac{1}{2}$ to

$$\overline{r_i'} = \bar{r}_i' = \frac{-4\omega_i^2\zeta_i + \epsilon_{i,\mathrm{lin}}\sin(2\bar{\psi}_i)}{8\omega_i^2}\bar{r}_i + \frac{\epsilon_{i,\mathrm{nlin}}\sin(2\bar{\psi}_i)}{16\omega_i^2}\bar{r}_i^3, \tag{12a}$$

$$\overline{\psi_i'} = \bar{\psi}_i' = \frac{-\frac{3}{2}\frac{\kappa_i^2}{\omega_i}\,\Delta\Omega\,\bar{r}_i^2 - 2\,\Delta\Omega\,\omega_i + \frac{3}{2}\kappa_i^2\bar{r}_i^2 + \epsilon_{i,\mathrm{lin}}\cos(2\bar{\psi}_i) + \cos(2\bar{\psi}_i)\bar{r}_i^2\epsilon_{i,\mathrm{nlin}}}{8\omega_i^2}. \tag{12b}$$

For a limit cycle the averaged changes $\bar{(\ )}'$ of both r_i and ψ_i have to be zero over one period of the vibration. Neglecting any damping ($\zeta_i = 0$), the solutions are [3, 8][1]:

[1] Equations 13b-d are similar to equations 16-19 and 22&23 in [8]. However, a different normalisation with different parameters is chosen in [8].

$$\bar{r}_\mathrm{a} = 0 \qquad \wedge \quad \bar{\psi}_\mathrm{a} = \frac{\arccos\left(\frac{2\omega_i}{\epsilon_{i,\mathrm{lin}}}\Delta\Omega\right)}{2}, \tag{13a}$$

$$\wedge \quad \bar{r}_\mathrm{b} = \pm\sqrt{\frac{4\omega_i\Delta\Omega + 2\epsilon_{i,\mathrm{lin}}}{-2\epsilon_{i,\mathrm{nlin}} + 3\kappa_i^2(1-\frac{\Delta\Omega}{\omega_i})}} \quad \wedge \quad \bar{\psi}_\mathrm{b} = \frac{\pi}{2}(1+2k),\ k \in \mathbb{N}, \tag{13b}$$

$$\wedge \quad \bar{r}_\mathrm{c} = \pm\sqrt{\frac{4\omega_i\Delta\Omega - 2\epsilon_{i,\mathrm{lin}}}{2\epsilon_{i,\mathrm{nlin}} + 3\kappa_i^2(1-\frac{\Delta\Omega}{\omega_i})}} \quad \wedge \quad \bar{\psi}_\mathrm{c} = \pi k,\ k \in \mathbb{N}, \tag{13c}$$

$$\wedge \quad \bar{r}_\mathrm{d} = \pm\sqrt{\frac{-2\epsilon_{i,\mathrm{lin}}}{\epsilon_{i,\mathrm{nlin}}}} \qquad \wedge \quad \bar{\psi}_\mathrm{d} = \frac{\arccos\left(\frac{3\kappa_i^2}{\epsilon_{i,\mathrm{nlin}}}(\frac{\Delta\Omega}{\omega_i}-1) - \frac{2\omega_i}{\epsilon_{i,\mathrm{lin}}}\Delta\Omega\right)}{2}. \tag{13d}$$

2.4. Bifurcation analysis

Each pair of amplitudes in equation 13b-d represents the same physical response. The period of $z_i(\tau)$ is $T = 4\pi$ and hence $\bar{r}_{b/c/d+}(\tau) = \bar{r}_{b/c/d-}(\tau + 2\pi)$. The limit cycles (equations 13b&c) bifurcate from the trivial steady state equation 13a at the bifurcation points

$$\Delta\Omega = \mp\Delta\Omega_{\mathrm{b},1} = \mp\frac{\epsilon_{i,\mathrm{lin}}}{2\omega_i}. \tag{14}$$

Equation 13a, describing the system's rest position, is unstable in between these points, if $\zeta_i < 2\epsilon_{i,\mathrm{lin}}$. In this case the trivial steady state is unstable/stable according to whether the bifurcated limit cycle is stable/unstable. Also, the eigenvalues of the Jacobian evaluated at the branch point are $\lambda = 0$ with multiplicity 2. The bifurcations thus have the characteristic of saddle-node bifurcations with the unstable state as the repelling saddle and the stable one as the attracting node (see [12] for example).

The stability of the limit cycles equations 13b,c at the bifurcation points depend on whether they have hardening or softening amplitude characteristics $\bar{r}_\mathrm{b}$ or $\bar{r}_\mathrm{c}$, respectively. The hardening or softening behaviour is determined by the non-linearity parameter κ_i^2 as shown in figure A1.

The stability of the bifurcated limit cycles equations 13b,c changes at

$$\Delta\Omega_{\mathrm{b},2} = \frac{\omega_i\epsilon_{i,\mathrm{lin}}\epsilon_{i,\mathrm{nlin}} - 3\kappa_i^2\omega_i\epsilon_{i,\mathrm{lin}}}{2\omega_i^2\epsilon_{i,\mathrm{nlin}} - 3\kappa_i^2\epsilon_{i,\mathrm{lin}}}, \quad \Delta\Omega_{\mathrm{b},3} = \frac{-\omega_i\epsilon_{i,\mathrm{lin}}\epsilon_{i,\mathrm{nlin}} - 3\kappa_i^2\omega_i\epsilon_{i,\mathrm{lin}}}{2\omega_i^2\epsilon_{i,\mathrm{nlin}} - 3\kappa_i^2\epsilon_{i,\mathrm{lin}}} \tag{15}$$

where both are connected via the unstable limit cycle equation 13d (see figure A1).

As mentioned in section 2.1 the stiffness constants $k_{\mathrm{PE},i,\mathrm{lin}}$ have an effect on the natural frequencies which drift, if the PE is not kept at a constant level. Furthermore, such transient PE behaviour also affects κ^2. This can cause changes in the system's qualitative behaviour when varying the level of the PE.

3. Semi-analytical and numerical validation

For a numerical validation parameters are introduced for a 2DOF system according to figure 1. Physical and quasi-modally transformed parameters are stated in table A1 and table A2 in the appendix. For approximating the limit cycles of equations 9 damping was neglected. To investigate this effect on the analytical solutions (equations 13), equations 12 are evaluated numerically in section 3.1. For validating the accuracy of both steps of the approximation, which are the approximation of the 2DOF system with 1DOF models and the averaging method, the original equations 7 are assessed numerically in section 3.2. These numerical results then are compared to the analytical results of sections 2.3 and 3.1.

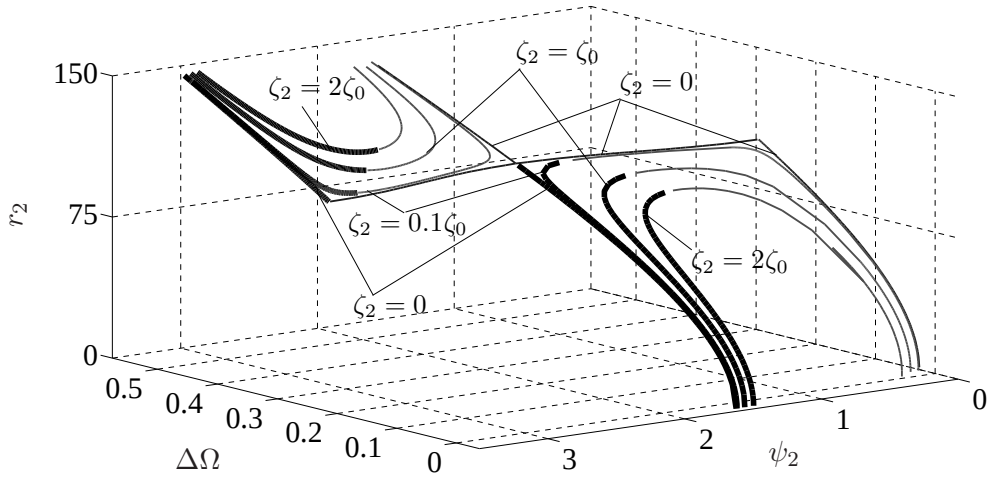

Figure 2. Reduced parameter-phase-space $\Delta\Omega$-ψ_1-r_1: Analytical (no damping: $\zeta_1 = 0$) and semi-analytical (for different damping ratios ζ_1) solutions of equations 12 at the first PR for parameters in table A2. The value ζ_0 denotes a damping ratio as stated in table A2. Bold: stable states, thin: unstable states.

3.1. Numerical evaluation of the averaged equations

Equations 12 are set equal to zero leaving an algebraic set of equations. These equations are solved numerically employing the homotopy method. The results for parameters as stated in table A2 and different values of ζ are compared to the analytical results equations 13 (see figure 2). Including damping connects the limit cycles equations 13b-d to two loops. Reducing the amount of damping being present, the amplitudes and phase shifts of the limit cycles approach equations 13b-d asymptotically. Since this approach solves the analytically averaged equations numerically, it is referred to as *semi-analytical* approach in the following.

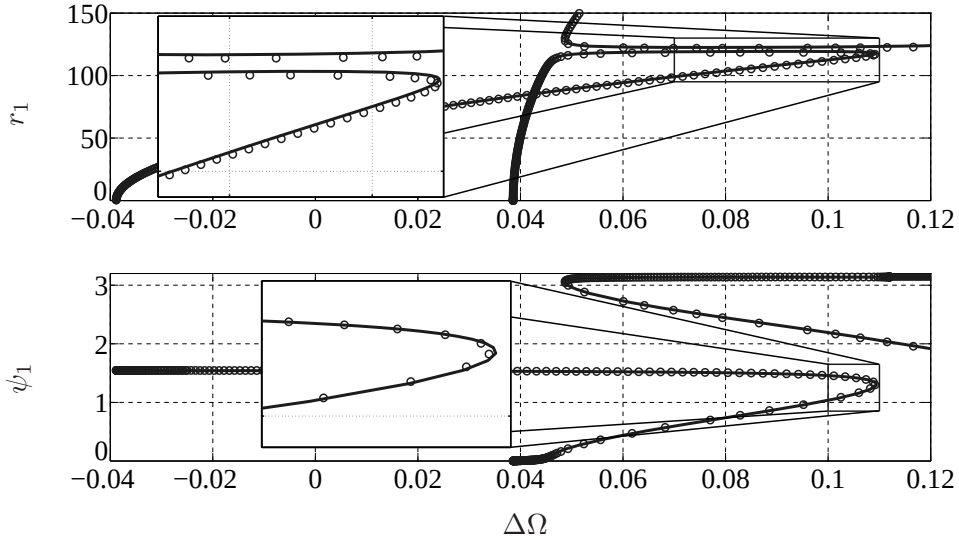

Figure 3. Numerical continuation, first quasi-modal displacement z_1, first PR ($\Omega_0 = 2\omega_1$). Original 2DOF model (line) and reduced 1DOF model (circles). The boxes zoom in on the turning points of the loops where the difference between the results is at a maximum.

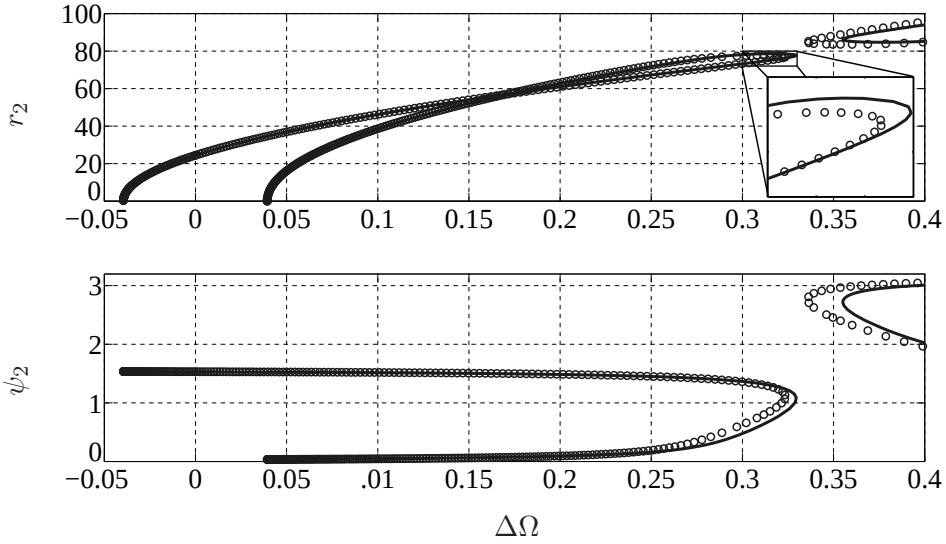

Figure 4. Numerical continuation, second quasi-modal displacement z_2, second PR ($\Omega_0 = 2\omega_2$). Original 2DOF model (line) and reduced 1DOF model (circles). The box zooms in on the turning point of the loop where the difference between the results is at a maximum.

3.2. Numerical validation of the analytical approximation

For the numerical continuation the MATLAB package MATCONT [13] is employed. First the accuracy of the quasi-modal reduction is tested. Comparing continuation results for the original equations 7 and the quasi-modally to 1DOF reduced equation 9, very close agreement can be observed at both PRs (see figure 3 and 4). This proves that, at least for the parameter set in table A1, the quasi-modal reduction holds a very good approximation for the behaviour at PR. However, at the second PR the phase shift ψ_2 is slightly overestimated close to the turning point of the loop on the left hand side and slightly underestimated close to the turning point of the loop on the right hand side.

Indeed, the analytical estimate of the limit cycles (equations 13) uses two more approximations: first averaging over one period of the limit cycle and second neglecting any damping. Yet, comparing the continuation results of the original equations 7 with the continuation of the quasi-modally reduced and averaged equations 12 and the approximations (equations 13) show very close agreement within both PR intervals. Within the instability interval of the rest position ($\Delta\Omega 0 = \mp 0.0387$ and $\Delta\Omega 0 = \mp 0.0396$, respectively) the three different approaches lead to almost identical results. For larger values of $\Delta\Omega$ the results differ more from each other (see figures 5 and 6). For the first PR this inaccuracy does not result from approximating the 2DOF system with an 1DOF model as shown earlier (see figure 3), but solely because the influence of higher order terms was neglected in the analytical and semi-analytical approach. Hence the non-linear softening behaviour is underestimated for large magnitudes of z_1. For the the second PR ($\Omega_0 = 2\omega_2$) the difference between the approaches is partly caused by neglecting higher order terms for the approximation. But in addition, approximating the 2DOF system with an 1DOF model causes some inaccuracies (see figure 4). Thus, the estimation of the amplitudes and phase shifts of the limit cycles is better at the first PR.

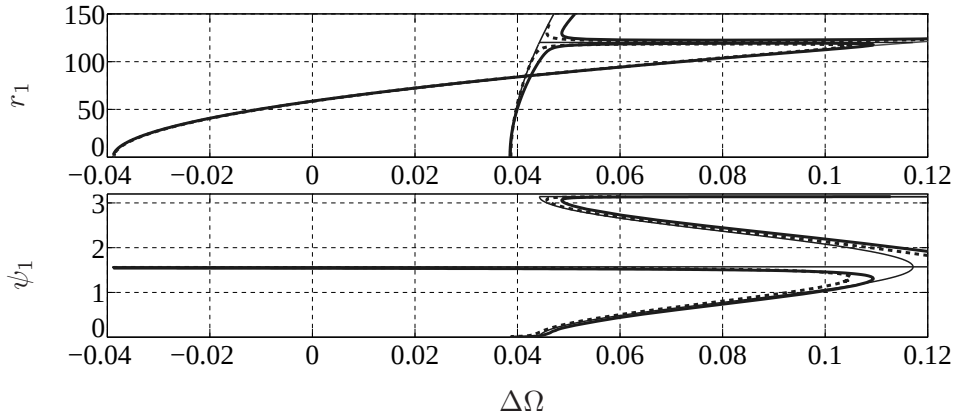

Figure 5. Limit cycles of equation 9 for the first quasi-modal displacement $z_1(t)$ at the first PR ($\Omega_0 = 2\omega_1$). Thin: analytical approximation, bold and dashed: semi-analytical approximation, bold and solid: numerical solution.

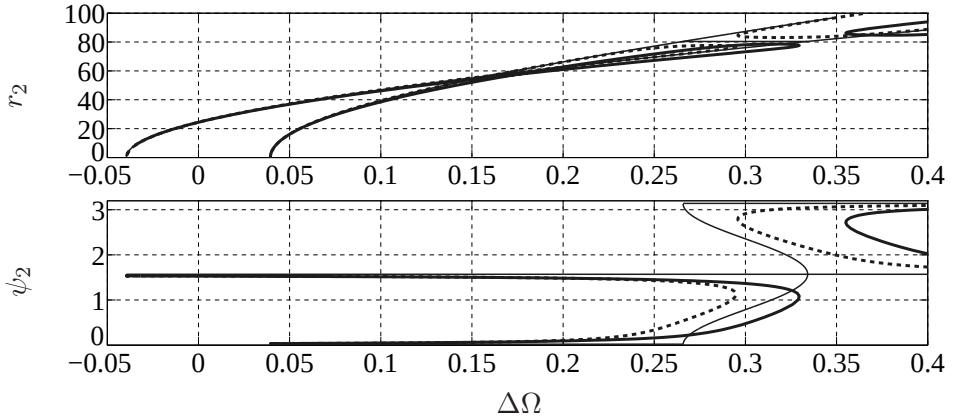

Figure 6. Limit cycles of equation 9 for the second quasi-modal displacement $z_2(t)$ at the second PR ($\Omega_0 = 2\omega_1$). Thin: analytical approximation, bold and dashed: semi-analytical approximation, bold and solid: numerical solution.

4. Conclusion

Investigating MDOF non-linear PE systems analytically is no straightforward process and certainly requires some basic understanding of effects of PE. But quasi-modally transforming the model enables one to concentrate on the important mode at a certain PR. For this mode the model can be reduced to 1DOF by a numerical transformation. The behaviour of this 1DOF non-linear PE model can be approximated via an averaging according to Krylov-Bugolyubov. Five different regimes of the non-linearity parameter can be identified leading to different qualitative behaviours. With this knowledge MDOF PE systems can be designed and tuned very easily and very time-efficiently with little computational effort. For the presented example the accuracy of the analytical approximation is excellent within the PRs and reasonable good (less than 10% error) for nearby frequencies within a interval up to five times the bandwidth of the PR.

Acknowledgments

The research efforts leading to the presented results were supported by a One-year Grant for Doctoral Candidates by the German Academic Exchange Service (DAAD) and a Marietta Blau Grant by the Austrian Ministry of Science, Research and Economy (BMWFW) for the lead author.

Appendix

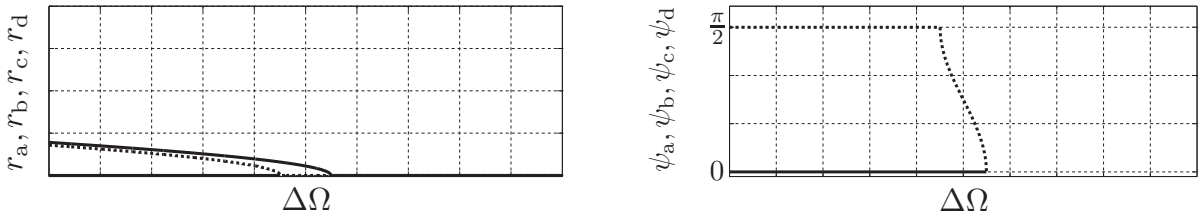

(a) Amplitudes and phase shifts of the limit cycles for $\kappa^2 = -0.4$.

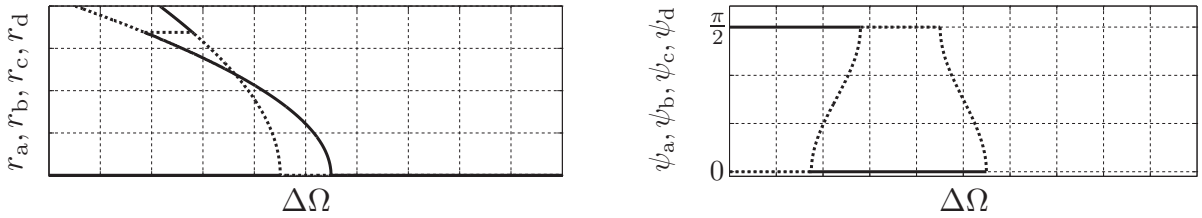

(b) Amplitudes and phase shifts of the limit cycles for $\kappa^2 = -0.01$.

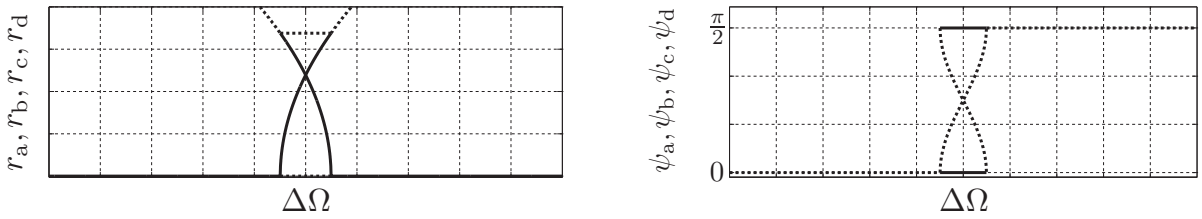

(c) Amplitudes and phase shifts of the limit cycles for $\kappa^2 = 0$.

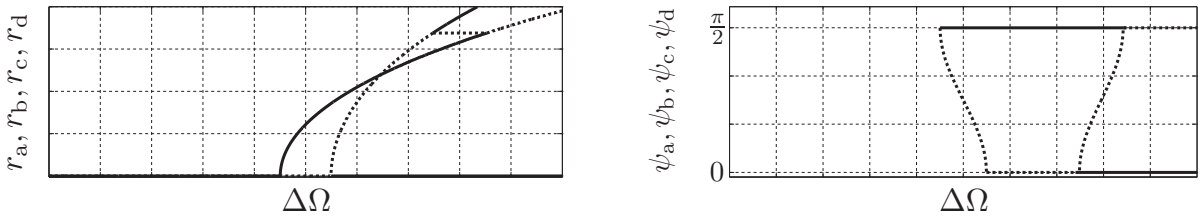

(d) Amplitudes and phase shifts of the limit cycles for $\kappa^2 = -0.01$.

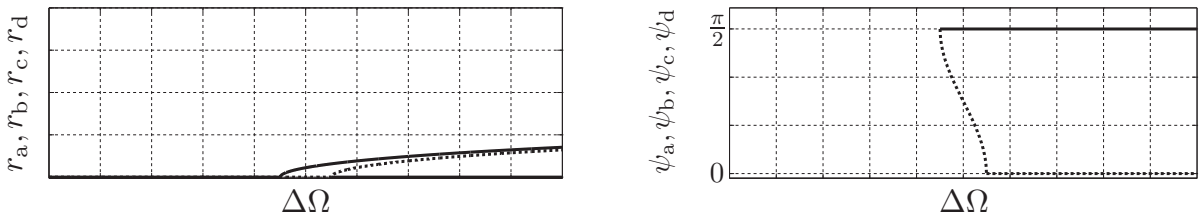

(e) Amplitudes and phase shifts of the limit cycles for $\kappa^2 = -0.4$.

Figure A1. The hardening/softening behaviour as well as the stability of the bifurcating limit cycles depends on κ^2. Five different regimes can be identified: (a)+(e): $|\kappa^2| > \left|\frac{4\epsilon_{\mathrm{nlin}}\omega_0}{3\epsilon_{\mathrm{lin}}}\right|$, (c):$-\left|\frac{4\epsilon_{\mathrm{nlin}}\omega_0^2}{3(\epsilon_{\mathrm{lin}}+2\omega_0^2)}\right| < \kappa^2 < \left|\frac{4\epsilon_{\mathrm{nlin}}\omega_0^2}{3(\epsilon_{\mathrm{lin}}-2\omega_0^2)}\right|$, (b)+(d): else. Solid: stable states, dashed: unstable states.

Table A1. Physical parameters of the 2DOF system introduced in section 3.

Parameter	Symbol	Value	Unit
Mass	m_1	$1.22 \cdot 10^{-10}$	kg
	m_2	$2.44 \cdot 10^{-10}$	kg
Damping	c_{01}	$1.94 \cdot 10^{-8}$	$\mathrm{N\,m^{-1}\,s}$
	c_{12}	$0.97 \cdot 10^{-8}$	$\mathrm{N\,m^{-1}\,s}$
	c_{12}	$1.94 \cdot 10^{-8}$	$\mathrm{N\,m^{-1}\,s}$
Linear Stiffness	$k_{01,\mathrm{lin}}$	3.505	$\mathrm{N\,m^{-1}}$
	$k_{12,\mathrm{lin}}$	1.753	$\mathrm{N\,m^{-1}}$
	$k_{02,\mathrm{lin}}$	3.505	$\mathrm{N\,m^{-1}}$
Non-linear Stiffness	$k_{01,\mathrm{nlin}}$	$18 \cdot 10^9$	$\mathrm{N\,m^{-3}}$
	$k_{12,\mathrm{nlin}}$	$9 \cdot 10^9$	$\mathrm{N\,m^{-3}}$
	$k_{02,\mathrm{nlin}}$	$18 \cdot 10^9$	$\mathrm{N\,m^{-3}}$
Linear PE Stiffness	$k_{\mathrm{PE},1,\mathrm{lin}}$	0.2281	$\mathrm{N\,m^{-1}}$
	$k_{\mathrm{PE},2,\mathrm{lin}}$	0.2281	$\mathrm{N\,m^{-1}}$
Non-linear PE Stiffness	$k_{\mathrm{PE},1,\mathrm{nlin}}$	$-1.056 \cdot 10^{10}$	$\mathrm{N\,m^{-3}}$
	$k_{\mathrm{PE},2,\mathrm{nlin}}$	$-1.056 \cdot 10^{10}$	$\mathrm{N\,m^{-3}}$

Table A2. Quasi-modally transformed, dimensionless parameters of the 2DOF system introduced in section 3 for modelling the system with the 1DOF model equation 9.

Non-dimensional Parameter	Symbol	Value
Natural Angular Frequencies	ω_1	1.3628
	ω_2	2.2109
Eigenmodes	$\boldsymbol{\varphi}_1$	$\begin{pmatrix} 3.2524 \\ 5.9745 \end{pmatrix} 10^4$
	$\boldsymbol{\varphi}_2$	$\begin{pmatrix} 8.4492 \\ -2.2998 \end{pmatrix} 10^4$
Modal Damping Ratios	ζ_1	$3.7715 \cdot 10^{-4}$
	ζ_2	$6.1187 \cdot 10^{-4}$
Non-linearity Parameters	κ_1^2	$1.0806 \cdot 10^{-5}$
	κ_2^2	$15.827 \cdot 10^{-5}$
Linear PE Parameters	$\epsilon_{1,\mathrm{lin}}$	0.10555
	$\epsilon_{2,\mathrm{lin}}$	0.17490
Non-linear PE Parameters	$\epsilon_{1,\mathrm{nlin}}$	$-1.4636 \cdot 10^{-5}$
	$\epsilon_{2,\mathrm{nlin}}$	$-5.4113 \cdot 10^{-5}$
Scaling Parameter	**Symbol**	**Value**
Frequency Scaling Parameter	Ω^*	$10^5\,\mathrm{s^{-1}}$
Displacement Scaling Parameter	x^*	$10^{-6}\,\mathrm{m}$

References

[1] Tondl A 1998 To the problem of quenching self-excited vibrations *Acta Technica CSAV* **43**(1) 109–16
[2] Ecker H and Pumhössl T 2012 Vibration suppression and energy transfer by parametric excitation in drive systems *Proc. IMechE Part C: J. Mech. Eng. Sc.* **226**(8) 2000–14
[3] Kniffka T J and Ecker H 2015 Parametrically excited microelectromechanical systems (MEMS) *e & i Elektrotechnik und Informationstechnik* **132**(8) 456–61
[4] Welte J, Kniffka T J and Ecker H 2013 Parametric excitation in a two degree of freedom MEMS system *Shock and Vibration* **20** 1113–24
[5] Dohnal F and Mace B R 2008 Amplification of damping of a cantilever beam by parametric excitation *Proc. MOVIC 2008* (Southampton: Univ. of Southampton, Inst. of Applied Mechanics) 1248
[6] Jia Y, Yan J, Soga K and Seshia A A 2013 Parametrically excited MEMS vibration energy harvester with design approaches to overcome the initiation threshold amplitude *J. Micromech. Microeng.* **23** 114007
[7] Zhang W, Baskaran R and Turner K L 2002 Effect of cubic nonlinearity on autoparametrically amplified resonant MEMS mass sensor *Sensors and Actuators A* **102** 139–50
[8] Rhoads J F, Shaw S W, Turner K L, Moehlis J, DeMartini B E and Zhang W 2006 Generalized parametric resonance in electrostatically actuated microelectromechanical oscillators *J. Sound Vib.* **296** 797–829
[9] Kniffka T J, Welte J and Ecker H 2012 Stability analysis of a time-periodic 2-dof MEMS structure *AIP Conf. Proc.* **1493** 559–66
[10] Kniffka T J and Ecker H 2013 Observations regarding numerical results obtained by the Floquet-method *Proc. ASME IDETC/CIE* (Portland: ASME) DETC2013/MSNDC-13292
[11] Krylov N M and Bogolyubov N N 1947 *Introduction to non-linear mechanics* (Princeton: Princeton Univ. Press)
[12] Kuznetsov Y A 1998 *Elements of applied bifurcation theory* 2nd edition (New York: Springer)
[13] Govaerts W, Kutznetsov Y A and Dhooge A 2005 Numerical continuation of bifurcations of limit cycles in MATLAB *SIAM J. Sci. Comput.* **27**(1) 231–52